This article has been accepted for publication in a future issue of this journal, but has not been fully edited. Content may change prior to final publication. Citation information: DOI 10.1109/TPEL.2018.2804658, IEEE Transactions on Power Electronics

Dynamic Power Management System Employing Single Stage Power Converter for Standalone Solar PV Applications

Anand I, Subramaniam Senthilkumar, *Member, IEEE,* Dipankar Biswas and M. Kaliamoorthy

***Abstract*—This paper presents a dynamic power flow management system for a solar PV system employing a single stage single inductor based dual input/output DC-DC converter feeding standalone DC loads backed up by a rechargeable battery. A time sharing voltage mode control scheme has been proposed for power flow management between solar PV, battery and standalone DC load and also it maintains a constant DC load voltage and performs MPPT operation of solar PV. The implementation of the control scheme has been described in detail. The steady state performance of the single stage converter has been explained with the relevant analytical expressions derived along with the characteristics. A state space average model was developed for simulating the transient behaviour and validating the working of the system for step changes in the input solar PV power and the DC loads. A hardware prototype of the proposed system has been fabricated and the proposed controller have been implemented using dSPACE DS1103 Real Time Interface(RTI) board. The working of the proposed scheme for the different levels of input solar insolation and DC Load power demand has been satisfactorily demonstrated and the corresponding results are also provided.**

***Index Terms*—DC-DC power conversion, Batteries, Solar power generation, Power converter, Multiport circuits and Photovoltaic power systems**

I. Nomenclature

C_{in}	Input capacitance of the proposed converter, μF
C_o	Output capacitance of the proposed converter, μF
D_{D1}	Duty ratio of the diode D_1
D_{Din}	Duty ratio of the diode D_{in}
$D_{S_{boost}}$	Duty ratio of boost switch S_{boost} of the proposed converter
D_{S2}	Duty ratio of the diode S_2
D_{S3}	Duty ratio of switch S_3
D_{Din}	Duty ratio of the input diode of the proposed converter.
P_{load}	Standalone DC Load power, W
P_{pv}	Solar PV Module power output, W
V_{mpp}	Voltage of solar PV module at maximum power point, V
V_{bat}	Terminal voltage of the Battery, V
V_o^*	Reference voltage of the standalone DC load, V

II. Introduction

Anand I, Subramaniam Senthilkumar and Deepankar Biswas are with National Institute of Technology, Tiruchirappalli (contact: 407114008@nitt.edu, skumar@nitt.edu and dipankrbiswas1992@gmail.com).

Kaliamoorthy M is with Dr. Mahalingam College of Engineering and Technology, India (contact: kaliasgoldmedal@gmail.com)

HARNESSING renewable energy sources such as wind energy, solar energy, tidal, etc. is critical for overcoming problems due to global warming and environmental degradation caused by the use of fossil fuels. Among all renewable energy sources, solar PV is abundant, has high power density, is modular and scalable. Solar PV is used both in grid connected applications and standalone applications. It can be used in a wide range of applications from a microwatt internet of things (IoT) system to a megawatt scale solar PV plant [1], [2]. Solar PV operates in a wide range of DC voltages, while electrical and electronic systems also have different levels of DC voltage requirements [3]. Hence, it is necessary to use power electronic interfaces for solar PV applications.

Since the energy from solar PV is intermittent in nature, it is necessary to combine energy storage systems and other renewable energy sources to maintain reliable operation for standalone PV systems. This can be achieved by many single input/output (dual port) DC-DC converters in parallel or multiport DC-DC converters. The centralized architecture of multiport converters uses fewer switches, has compact structure, lower cost, higher efficiency and avoids the need to use communication systems as compared to multiple single input/output DC-DC converters [4], [5] and [6].

Sun *et al.* [4] have proposed a three port converter incorporating solar PV, battery as power sources feeding DC loads with galvanic isolation. The control structure involved a complex hybrid modulation technique (PWM + PFM) with soft switching. Ray *et al.* proposed an integrated dual output DC-DC converter which had both buck and boost outputs using PWM to regulate output voltages [7]. Various possible topologies for multiport converters have been discussed in [8]. However, using multiple inductors results in large converter size and cost. In order to overcome these problems, single inductor multiple input/output topologies have been proposed. Single inductor multiple ouput DC-DC converters based on buck, buck-boost and boost topologies have been proposed in various literature [9], [10], [11], [12] and [13]. This reduces the cost, circuit complexity and results in greater efficiency.

Nami *et al.* [14] have proposed single input multi output boost converters based on diode clamped topology for multiple series and multiple parallel outputs using cascaded voltage and current control loops. Khaligh *et al.* [15] have proposed a single inductor based multi input bidirectional DC-DC converter which operates in buck, boost and

This article has been accepted for publication in a future issue of this journal, but has not been fully edited. Content may change prior to final publication. Citation information: DOI 10.1109/TPEL.2018.2804658, IEEE Transactions on Power Electronics

buck-boost mode. Various non-isolated single inductor multi input/output topologies have been reviewed in [16]. Isolated converters are used when there is a requirement for high step up ratio and galvanic isolation. But the drawbacks are larger size and complexity compared to non-isolated converter topologies. Single inductor multi input multi output topologies, which are a hybrid of multi input and multi output converters utilizes multiple power sources to supply power to multiple applications [10],[17],[18],[19] and [20].

Bandyopadhyay and Chandrakasan [10] present a multi input multi output DC-DC converter utilizing three different power sources namely piezoelectrics, solar PV and thermoelectric for low voltage applications. Huang and Chen [17], presented a multi input multi output DC-DC converter with buck and boost outputs for low power portable applications using hysteresis and PWM control. Shao *et al.* [18] presented a dual input/output DC-DC converter for low power applications using solar PV as power source and battery as energy storage device. Two modes of operation of the converter – dual input mode during deficit solar PV power and dual output mode during surplus solar PV power is presented. Babaei and Abbasi [19] proposed a switched capacitor based boost converter topology which is used for multiple outputs in series. A detailed analysis of the converter topology was carried out. Keyhani and Toliyat [20] proposed a zero voltage switching single inductor multi input multi output converter with buck-boost mode of operation.

This paper proposes a novel and simple time sharing closed loop control technique for solar PV system with a single inductor power converter stage, wherein the controller maintains a constant DC load voltage and a power flow management system to balance the power flow between solar PV, battery and stand-alone DC loads. The power converter is capable of operating in dual input/output mode controlled by an effective energy storage/energy management system for providing uninterrupted power supply to the standalone DC load from a battery to take care of both excess and deficit PV power availability situations. Steady state analysis is performed by deriving analytical expressions and the transient analysis by developing a state space average model of the proposed system. Starting with the description of the proposed system, steady state analysis, the simulated and experimental waveforms of various electrical quantities are presented in the succeeding sections.

III. Proposed Solar PV Power Flow Management System and Operation

The proposed system is shown in Fig. 1. It consists of a solar PV module as power source, battery as energy storage element to supply during absence of solar PV, a single inductor based dual input/output DC-DC converter feeding a standalone DC load and a controller which modulates power flow between a solar PV module, a battery and a standalone DC load and performs voltage regulation at the standalone DC load terminals. The various functional blocks of the proposed system is as follows:

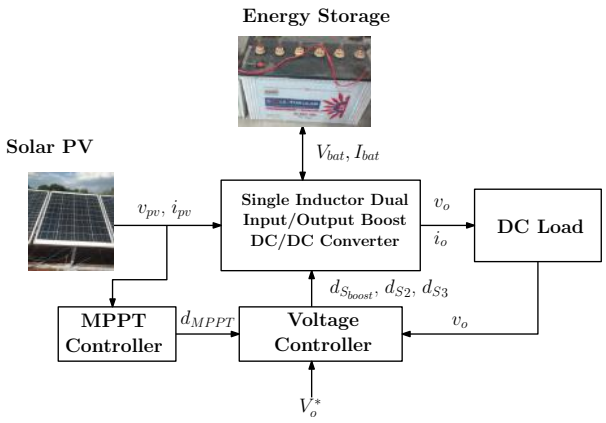

Fig. 1. Block diagram of proposed power flow management system

A. Solar PV Module

The solar PV module is the primary source of power for the standalone DC load. The power generated by the solar PV module for a given temperature and level of irradiation depends on PV voltage and current drawn by the load. Hence, in order to do load matching, a maximum power point tracking (MPPT) control is used to set the converter at maximum power point (MPP) by varying the duty ratio of the appropriate switch and hence the current drawn by the converter from the solar PV module. There are many algorithms used to track the MPP like constant voltage, perturb and observe, incremental conductance and beta method [21]. Among them, a simple perturb and observe (P&O) algorithm is selected for the proposed system.

A 24 V 60 W solar PV module is selected for the proposed system and the same is modelled using the five parameter model [22]. The output current of the solar PV module used in modelling is,

$$I_{pv} = I_L - I_o \left(e^{\frac{q(V+IR_s)}{nKT}} - 1 \right) \tag{1}$$

The key specifications of the solar PV module used are shown in TABLE I.

B. Energy Storage

Since the power from the solar PV module is intermittent, a rechargeable battery has to be used as an energy buffer to maintain continuous operation of the system. During times of surplus PV power, it stores excess energy and during times of deficit or absence of PV power, it complements or replaces

TABLE I
Parameters of the Solar PV Module at temperature 25°C

Open circuit Voltage (V_{oc})	32.8 V
Short circuit current (I_{sc})	2.6 A
Nominal voltage (V_{mpp})	24.65 V
Nominal Current (I_{mpp})	2.44 A
Maximum Power (P_{mpp})	60.3 W

This article has been accepted for publication in a future issue of this journal, but has not been fully edited. Content may change prior to final publication. Citation information: DOI 10.1109/TPEL.2018.2804658, IEEE Transactions on Power Electronics

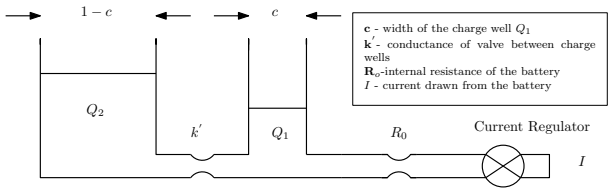

Fig. 2. Kinetic Energy Battery Model

the solar PV module as the power source. There are primarily two types of rechargeable batteries used for stationary power applications - the lead acid battery and the lithium ion battery. Since lead acid batteries are inexpensive and have less safety issues, it is used for the proposed system.

Jongerden and Haverkort have discussed various battery models [23]. For modelling of the system, Kinetic Battery Model, an intuitive battery model based on electrical elements is selected. Lead acid batteries' Ampere hour capacity are rated for particular duration of discharge – typically 10 hour and 20 hour rates of discharge. If the battery is discharged faster than rated discharge, lesser amount of capacity is available and the battery has to be rested to recover the remaining charge. Kinetic battery takes this into account by modelling the lead acid battery into two charge wells – available charge with charge Q_1 and non-available charge Q_2 as shown in Fig. 2. The dynamic equations for the two charge wells are,

$$\frac{dq_1}{dt} = -I + k^{'}\left(h_2 - h_1\right) \tag{2}$$

$$\frac{dq_2}{dt} = -k^{'}\left(h_2 - h_1\right) \tag{3}$$

The sum of the charges in the two charge wells gives the total remaining charge in the battery.

C. Single Inductor Based Dual Input/Output DC-DC converter

The boost derived single inductor based dual input/output DC-DC converter (SI-DIO) used in the proposed power flow management system is shown in Fig. 3. It consists of diode D_{in} which interfaces the solar PV module to the converter and also prevents reverse power flow to the solar PV module. The capacitor C_{in} is connected in parallel to the solar PV module to reduce the solar PV voltage ripples. The switches S_2 and diode D_2 is used to set the battery as an output to store excess solar PV power. The switch S_3 is used to set the battery as an input to supply power to the standalone DC load. The capacitor C_o is connected across the output to reduce the output voltage ripples.

The converter has two modes of operation namely dual output boost mode (DOBM) when the power from solar PV module exceeds DC load demand and dual input boost mode (DIBM) when there is a deficit. The circuit configuration for both the modes is shown in Fig. 4.

During DOBM, the solar PV module acts as a power source feeding the battery through the switch S_2 and the DC load through the diode D_1. The single inductor based dual

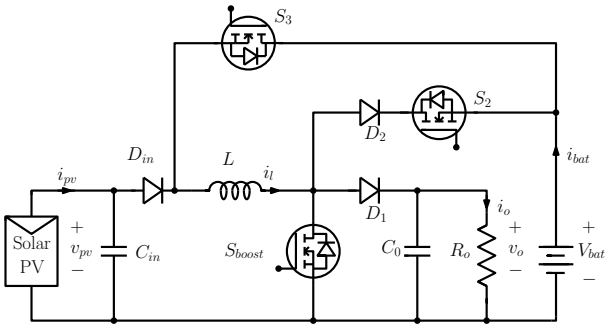

Fig. 3. Single Inductor based Dual input/output Boost DC-DC Converter

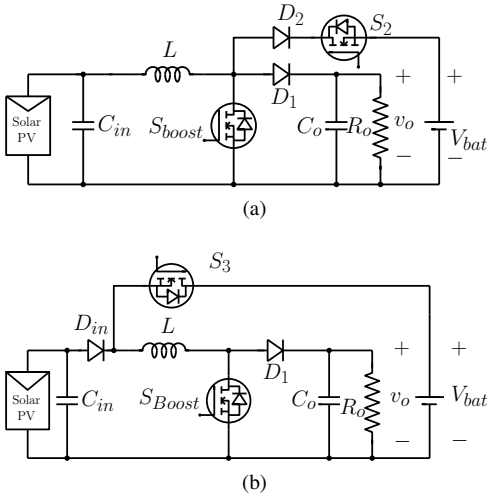

Fig. 4. Proposed single inductor based dual input/output DC-DC converter in (a) Dual Output Boost Mode(b) Dual Input Boost Mode

input/output DC-DC converter has three states as shown in Fig. 5. In the first state, the inductor is charged by power from the solar PV module through switch S_{boost}. In the second state, switch S_{boost} is turned off and the inductor discharges to the DC load through the diode D_1. In the third state, the surplus power is discharged to the battery by turning on the switch S_2. Since, the required voltage of the standalone DC load is higher than that of the battery, the diode D_1 is reverse biased and the standalone DC load is cut off. Typical waveforms for the inductor current i_l, the inductor voltage v_l, the battery current i_{bat} and the output DC load voltage v_o for this mode is shown in Fig. 5.

By volt second principle, the output DC load voltage of the converter in DOBM is obtained as,

$$V_o = \frac{V_{pv} - V_{bat}D_{S2}}{D_{D1}} \tag{4}$$

The equation is similar to the conventional boost converter equation, in which the effective input voltage is the difference between the solar PV module voltage v_{pv} and the pulse modulated fraction of the battery voltage, $V_{bat}d_{S2}$. The variation of standalone DC load voltage with respect to variation of duty cycles d_{D1} and d_{S2} for an input voltage of 24 V DC is observed in Fig. 6. It is seen that the standalone DC load voltage increases with either decrease in d_{D1} or by increasing d_{S2}. Rewriting eq. 4, the required input voltage

This article has been accepted for publication in a future issue of this journal, but has not been fully edited. Content may change prior to final publication. Citation information: DOI 10.1109/TPEL.2018.2804658, IEEE Transactions on Power Electronics

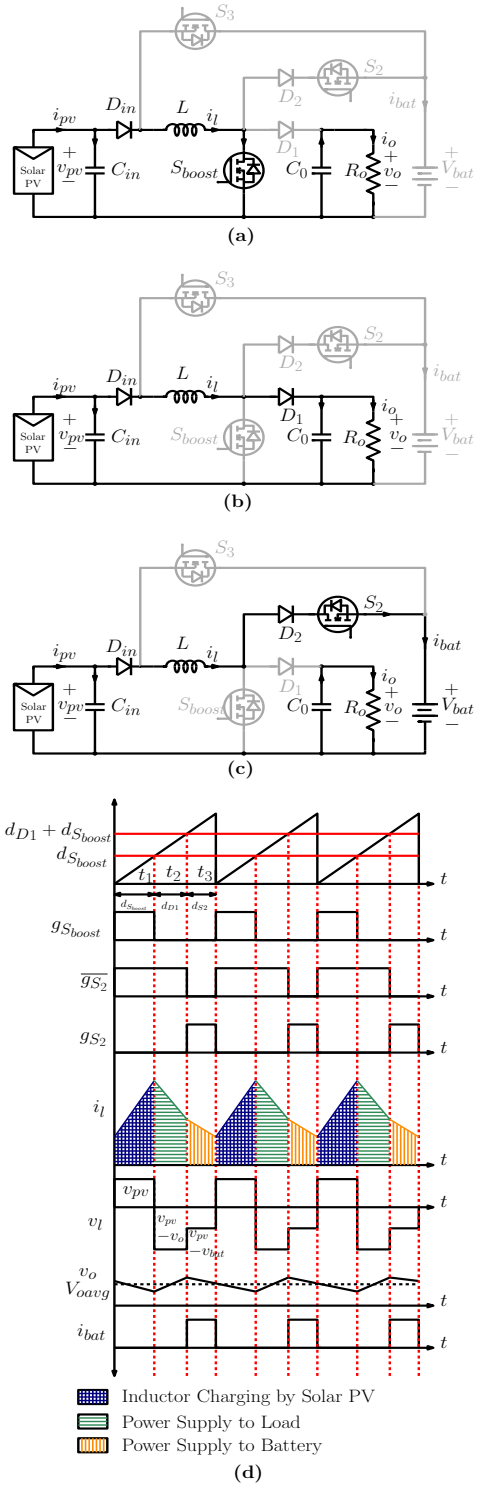

Fig. 5. Different circuit states in Dual Output Boost Mode (a) Charging of inductor by solar PV module (b) Discharge of inductor to standalone DC load (c) Discharge of inductor to battery (d) Typical waveforms during Dual Output Boost Mode

V_{pv} for various duty ratios d_{D1} and battery voltage V_{bat} for an specific output voltage of V_o can be calculated as,

$$V_{pv} = V_o D_{Din} + V_{bat} D_{S2} \tag{5}$$

The required input voltage and duty ratios for an specific output voltage of 48 V DC and a battery voltage of 36 V

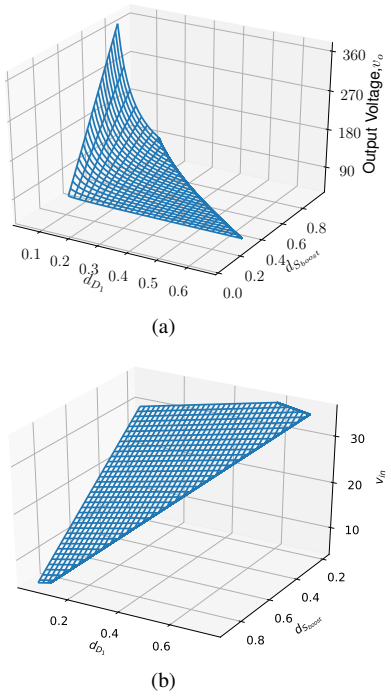

Fig. 6. Steady state Analysis in Dual Output Boost Mode (a) output voltage variation with changes in $d_{S_{boost}}$ and d_{Din} (b) Required input PV voltage for an DC load voltage of 48 V for various duty ratios of d_{Din} and $d_{S_{boost}}$

DC is plotted in Fig. 6.

The converter has been modelled by using the state space average model, developed by considering all the states of the circuit in DOBM as follows:

$$\begin{bmatrix} \frac{di_l}{dt} \\ \frac{dv_{pv}}{dt} \\ \frac{dv_o}{dt} \end{bmatrix} = \begin{bmatrix} 0 & \frac{1}{L} & -\frac{d_{D1}}{L} \\ -\frac{1}{C_{in}} & 0 & 0 \\ \frac{d_{D1}}{C_o} & 0 & -\frac{1}{C_o R_o} \end{bmatrix} \begin{bmatrix} i_l \\ v_{pv} \\ v_o \end{bmatrix} + \begin{bmatrix} \frac{d_{S2}}{L} & 0 \\ 0 & \frac{1}{C_{in}} \\ 0 & 0 \end{bmatrix} \begin{bmatrix} V_{bat} \\ i_{pv} \end{bmatrix} \tag{6}$$

where,

d_{D1} and d_{S2} are duty ratios of the diode D_1 and the switch S_2 respectively.

In the DIBM, the battery and the solar PV module act as input power sources for DC load. The switch S_3 sets the battery as an additional input power source. The single inductor based dual input/output DC-DC converter has four circuit states are shown in Fig. 7. In the first and second state, the inductor is charged by the solar PV module and the battery respectively. The switch S_{boost} is turned on for both the states. The switch S_3 is turned on for the second state to set the battery as the input power source. The diode D_{in} is reverse biased as the battery voltage is more than the voltage of the solar PV module. During the third and fourth circuit states, the switch S_{boost} is turned off and the inductor

This article has been accepted for publication in a future issue of this journal, but has not been fully edited. Content may change prior to final publication. Citation information: DOI 10.1109/TPEL.2018.2804658, IEEE Transactions on Power Electronics

discharges to the output. In the third circuit state, the battery is used as the power source by allowing the switch S_3 to remain on. During the fourth circuit state, the switch S_3 is turned off and the solar PV module becomes the power source. Typical waveforms for the inductor current i_l, the inductor voltage v_l, the battery current i_{bat} and the output voltage v_o for this mode is shown in Fig. 7.

By volt second principle, the standalone DC load V_o in DIBM is found as,

$$V_o = \frac{V_{pv} D_{Din} + V_{bat}\left(D_{S_{boost}} - D_{Din}\right)}{D_{S_{boost}}} \tag{7}$$

It is observed that the relationship is similar to the conventional boost converter equation in which the effective input voltage is the pulse modulated fraction of the input PV voltage and the battery voltage. The steady state output voltage for an PV voltage of 24 V DC and a battery voltage of 36 V DC is plotted in Fig. 8. The 3D plot shows that the output voltage increases linearly with increase in d_{S3} and exponentially with increase in $d_{S_{boost}}$.

The state space average model for DIBM has been developed by considering all the circuit states as follows:

$$\begin{bmatrix} \frac{di_l}{dt} \\ \frac{dv_{pv}}{dt} \\ \frac{dv_o}{dt} \end{bmatrix} = \begin{bmatrix} 0 & \frac{\overline{d_{S3}}}{L} & -\frac{\overline{d_{S_{boost}}}}{L} \\ -\frac{\overline{d_{S3}}}{C_{in}} & 0 & 0 \\ \frac{\overline{d_{S_{boost}}}}{C_o} & 0 & 0 \end{bmatrix} \begin{bmatrix} i_l \\ v_{pv} \\ v_o \end{bmatrix} + \begin{bmatrix} \frac{d_{S3}}{L} & 0 \\ 0 & \frac{1}{C_{in}} \\ 0 & 0 \end{bmatrix} \begin{bmatrix} V_{bat} \\ i_{pv} \end{bmatrix} \tag{8}$$

where,

$d_{S_{boost}}$, d_{S3} are the duty ratios of switches S_{boost} and S_3 respectively.

IV. Proposed Time Sharing Control Strategy

The overall time sharing control block diagram for the proposed power flow management system is shown in Fig. 9a. It consists of a proportional integral controller based voltage regulator to regulate the standalone DC load voltage of 48 V. The reference voltage (V_o^*) and the actual standalone DC load voltage (v_o) are given to an error amplifier, which gives the absolute standalone DC load error voltage (v_{oe}) and it is then converted to a per unit error voltage (v_{oepu}) by using the reference standalone DC load voltage as the base voltage. This per unit error voltage is the input for the PI controller. The output of the voltage regulator (d_{Volt}) modulates the power flow for DC load to address excess and deficit power based on the PV power availability by setting the appropriate mode of operation such as dual input boost mode (DIBM) and dual output boost mode (DOBM). A simple perturb and observe method is used for extracting the maximum power from the solar PV module by control signal d_{MPPT}.

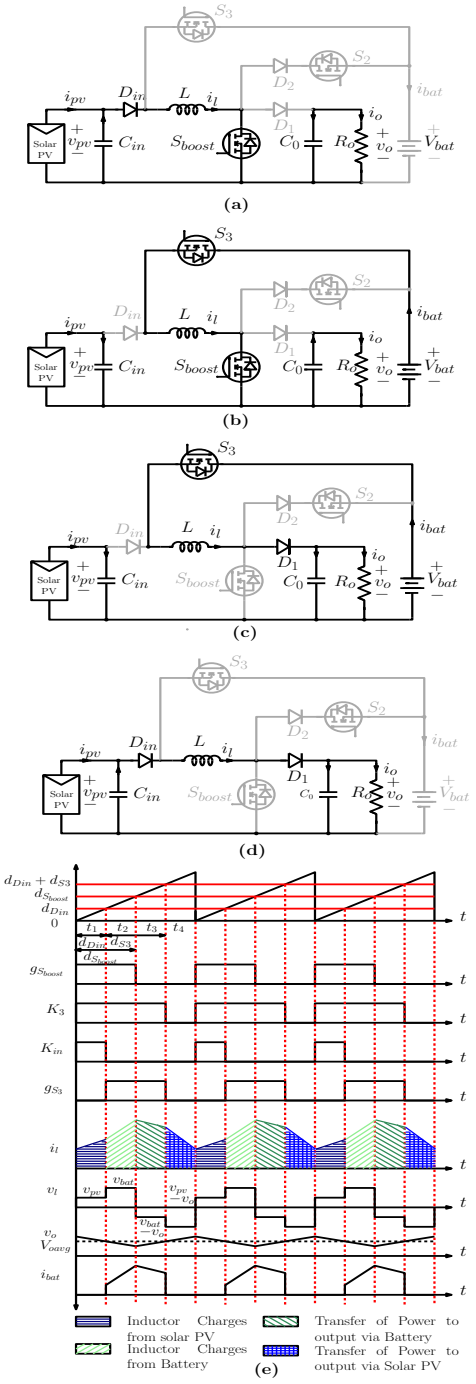

Fig. 7. Different Circuit states in Dual Input Boost Mode: (a) Charging of inductor by solar PV module (b) Charging of inductor by battery (c) Discharge of inductor to DC load with battery as power source (d) Discharge of inductor to output with solar PV module as power source (e) Typical waveforms during Dual Input Boost Mode

The mode change control decides the mode of operation of the converter by generating mode signal m_{sel} based on the standalone DC load power demand and the power extracted from the solar PV module. The rise in the standalone DC load voltage more than the standalone DC load reference voltage(V_o^*) shows the power extracted from the solar PV is more than the load power demand and vice versa, which confirms the operation of dual output/input

This article has been accepted for publication in a future issue of this journal, but has not been fully edited. Content may change prior to final publication. Citation information: DOI 10.1109/TPEL.2018.2804658, IEEE Transactions on Power Electronics

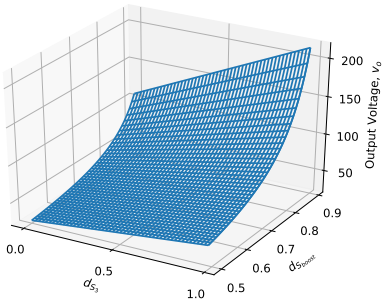

Fig. 8. Steady state Analysis in Dual Input Boost Mode - variation of output voltage for changes in d_{S3} and $d_{S_{boost}}$ for $v_{pv} = 24$ V and $V_{bat} = 36$ V

mode. The logic for the mode change signal is implemented by using logical and arithmetic operators. When the rise in the DC load voltage is 0.5 above V_o^* and the duty ratio d_{S3} is zero, the SR latch shown in figure is reset to zero, which sets the converter in DOBM. Similarly, when the fall in DC load voltage is 0.5 below V_o^* and the duty ratio d_{S2} is zero, the SR latch is set to one, which corresponds to DIBM.

The power modulation control controls the appropriate switches to perform the operation of the power converter in dual input/output mode based on control signals d_{Volt} and d_{MPPT} and the mode signal m_{sel} from mode change control by using arithmetic and logical operators. m_{sel} acts as one of the selector signals for the multiplexers. In DOBM, when there is excess solar PV power, MPPT is implemented by routing the MPPT control signal d_{MPPT} to $d_{S_{boost}}$ and the voltage regulation of standalone DC load is achieved by routing the voltage control signal d_{Volt} to d_{D1} by the multiplexers. The duty ratio d_{S2} is created by subtracting a constant of 1 with $d_{S_{boost}}$ and d_{D1}. The sequence of the duty ratios are shown in Fig. 5(d). The following expressions were implemented for the DOBM to operate the power switches S_{boost} and S_2.

$$d_{S_{boost}} = d_{MPPT} \tag{9}$$

$$d_{S2} = 1 - d_{D1} - d_{S_{boost}} \tag{10}$$

where,

$$d_{D1} = d_{Volt} \tag{11}$$

In DIBM, when there is deficit solar PV power, both voltage regulation and MPPT control is achieved by the switch $d_{S_{boost}}$. The MPPT control signal d_{MPPT} is routed to d_{Din} and the voltage regulation of the standalone DC load is achieved by routing the voltage control signal d_{Volt} to $d_{S_{boost}}$ through multiplexers. The sequence of the duty ratios is shown in Fig. 7(e). The duty ratio d_{S3} is obtained by subtracting $d_{S_{boost}}$ with d_{Din} and then dividing by $d_{S_{boost}}$. When the solar PV power becomes surplus, the duty ratio d_{S3} is slowly reduced to zero and the battery is cut off. This results in loss of MPPT as $d_{S_{boost}} = d_{Din} = d_{Volt}$. In order to regain control, MPPT control signal d_{MPPT} is routed to $d_{S_{boost}}$. A relational operator is used to detect this condition and generate the signal d_{sel} which acts as a select signal for the multiplexer for $d_{S_{boost}}$. The following expressions were implemented for the power switches S_{boost} and S_3 to operate the converter in DIBM.

$$d_{S_{boost}} = d_{Volt} \tag{12}$$

$$d_{Din} = d_{MPPT} \leq d_{S_{boost}} \tag{13}$$

$$d_{S3} = \frac{d_{S_{boost}} - d_{Din}}{d_{S_{boost}}} \tag{14}$$

From the outputs of the power modulation control ($d_{S_{boost}}$, d_{S2}, d_{S3}, d_{Din}) and the mode change signal, the gating pulses for the power switches $g_{S_{boost}}$, g_{S_2} and g_{S_3} are generated using the gate pulse generation block. A ramp signal v_{ramp} is used as a carrier signal for generating gate pulses. In DIBM, to generate firing pulses for switches S_{boost} and S_3 in the order as shown in Fig. 7, first the duty ratio $d_{S_{boost}}$ is compared with v_{ramp}. Since the gate signal g_{S_3} for the switch S_3 has to be generated between time period t_1 and t_2, it is generated in two steps. First, the two intermediate signals K_3 and K_{in} are generated. The signal K_3 is generated by summing up d_{Din} and d_{S3} and comparing with v_{ramp} and the signal K_{in} is generated by comparing d_{Din} with v_{ramp}. Next, the intermediate signals K_3 and K_{in} are XORed to get g_{S_3}. Similarly, for DOBM, the gate signal g_{Sboost} is generated by comparing $d_{S_{boost}}$ with v_{ramp}.

The DC load voltage control, MPPT and battery control are integrated by a time sharing voltage mode control. Each control is allocated a time slot to perform power flow as shown in Fig. 9a. During DOBM as shown in Fig. 9b, MPPT control decides the power drawn from the solar PV by controlling the switch S_{boost} with the duty ratio d_{MPPT}. This occurs from time period 0 to t_1. The voltage controller regulates power flow to the load by determining the period of conduction of diode D_1 (from t_1 to t_2) by controlling the duty ratio d_{Volt}. The surplus power flow to the battery is indirectly regulated by the voltage controller by turning on the switch S_2(from t_2 to t_3) for a duty ratio of d_{S2}. During DIBM as shown in Fig. 9c, the voltage controller controls the power power flow to the load by controlling the switch S_{boost} (from 0 to t_2) with a duty ratio of d_{Volt}. The MPPT control controls the power extracted from solar PV by determining the duration of conduction of diode D_{in} (from 0 to t_1) for a duty ratio of d_{MPPT}. The deficit power is made up by the battery by making it as a power source for a duty ratio of d_{S3} (from t_1 to t_3) which is determined by both voltage controller and MPPT controller according to eqn.14.

V. Results and Discussion

A. Simulation Results

The proposed power flow management system is simulated by implementing the state space model derived in equation(8) in the MATLAB/Simulink environment. The values of the passive elements used are 100 μH for boost inductor L, 1000 μF for input capacitor C_{in} and output capacitor C_o. A 60 W solar PV module with a MPP voltage of 24.5 V DC and MPP current of 2.44 A and a battery with 36 V DC are used as power sources. The reference voltage of the standalone DC load is set at 48 V DC. The PI

This article has been accepted for publication in a future issue of this journal, but has not been fully edited. Content may change prior to final publication. Citation information: DOI 10.1109/TPEL.2018.2804658, IEEE Transactions on Power Electronics

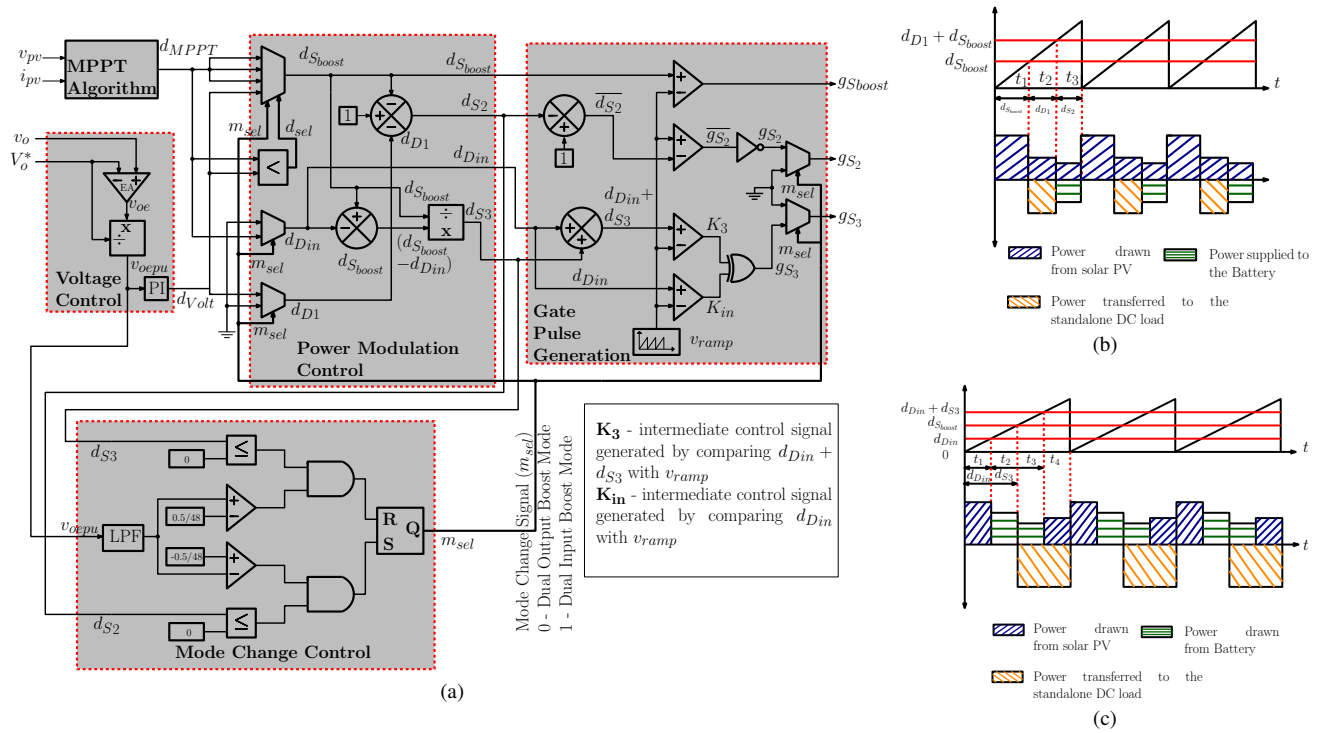

Fig. 9. Time sharing control scheme for proposed dynamic power flow management system (a) Schematic diagram (b) Power flow during Dual Output Boost Mode (c) Power flow during Dual Input Boost Mode

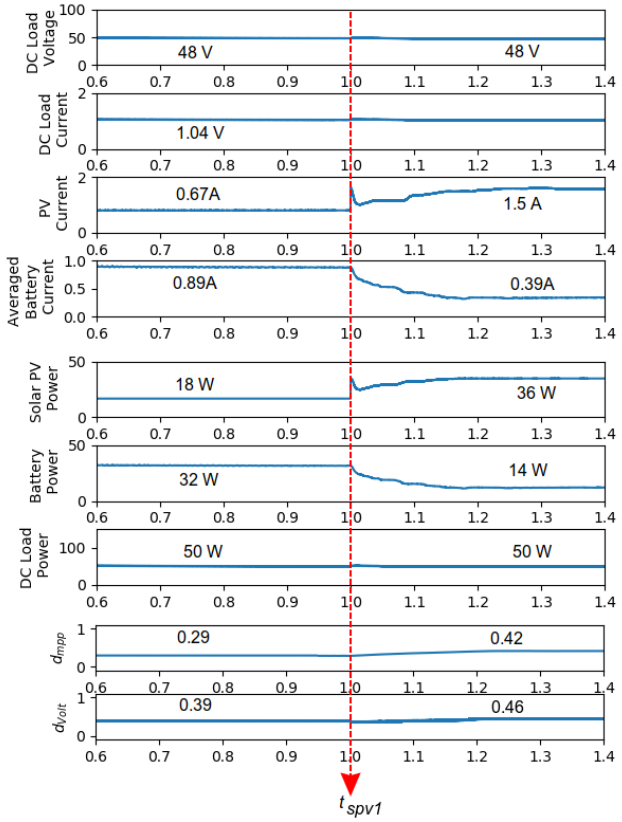

Fig. 10. Simulation of dynamic response of the converter to changes in PV power at t_{spv1}

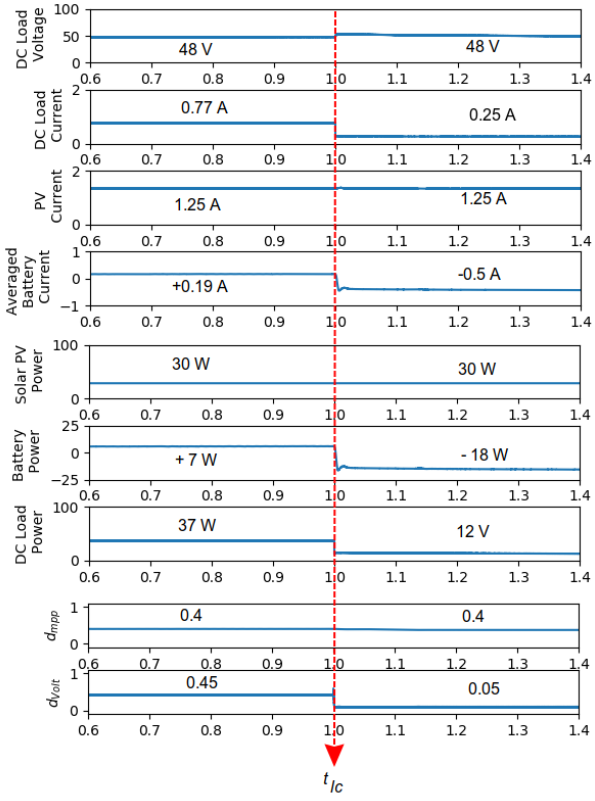

Fig. 11. Simulation of dynamic response of the converter to changes in standalone DC loadat t_{lc}

This article has been accepted for publication in a future issue of this journal, but has not been fully edited. Content may change prior to final publication. Citation information: DOI 10.1109/TPEL.2018.2804658, IEEE Transactions on Power Electronics

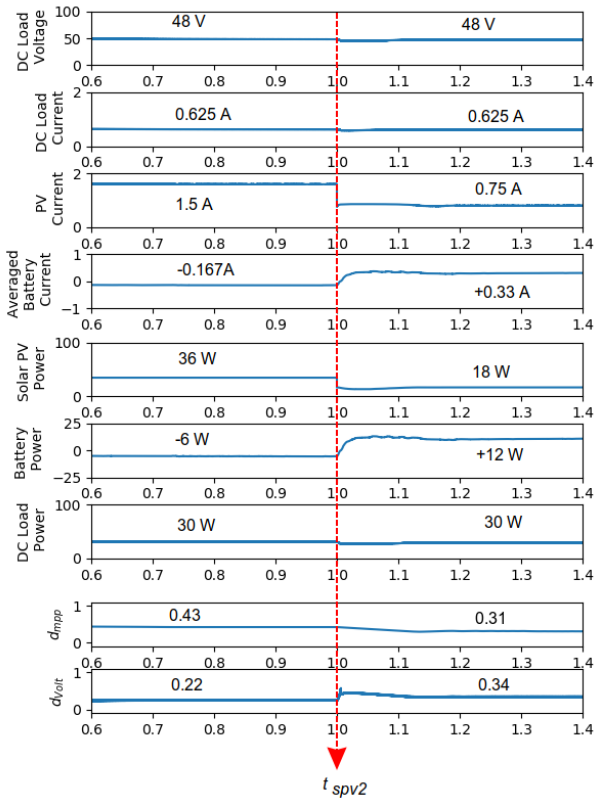

Fig. 12. Simulation of dynamic response of the converter to decrease in solar PV insolation at t_{spv2}

controller had values of $k_p = 5$ and $k_i = 15$ for per unit error input.

1) Case I: Increase in solar insolation from 300 W/$m^2$to 600 W/m^2: The power flow management system is initially operating in DIBM with a solar PV insolation of 300 W/m^2, capable of supplying 18 W. The standalone DC load power demand is 50 W. The MPPT control maintains a d_{MPPT} of 0.3 to extract 18 W from the solar PV module. The battery makes up for the power deficit of 32 W. At the time instant t_{spv1} shown in Fig. 10, the solar insolation level is increased to 600 W/m^2, making the solar PV module capable of supplying a power of 36 W. The MPPT algorithm increases the duty ratio d_{MPPT} to 0.4 to extract maximum power. Since the effective input voltage $V_{pv}D_{Din} + V_{bat}(D_{S_{boost}} - D_{Din})$ shown in eqn.7 decreases, the voltage controller increases the duty ratio d_{Volt} to maintain constant standalone DC load. Due to higher increase in d_{MPPT} compared to d_{Volt}, d_{S3} decreases in accordance with eqn. 14 and 13 and hence the share of the battery power to the DC load power demand reduces to 14 W.

2) Case II: Change in mode from DIBM to DOBM due to surplus power : Initially the power flow management system is operating at DIBM with solar PV and battery supplying a load demand of 37 W. At the time instant t_{lc}, as shown in Fig. 11 the standalone DC load power demand is decreased to 12 W. The voltage controller decreases d_{Volt} to regulate the standalone DC load voltage. When d_{Volt} becomes less than d_{MPPT}, maximum power point tracking control is lost as d_{Din} becomes less than d_{MPPT}. In this particular instant, the converter acts as a conventional boost converter with voltage control and the solar PV module as input. Hence in order to further extract power from the solar PV module, the controller shifts to MPPT by setting $d_{S_{boost}}$ equal to d_{MPPT}. This results in loss of voltage control and rise of load voltage above the reference voltage V_o^*. The mode change control shifts the converter to DOBM almost immediately. The controller reduces the duty ratio d_{D1} to reduce the standalone DC load voltage to V_o^* and duty ratio d_{S2} to divert excess power to batteries.

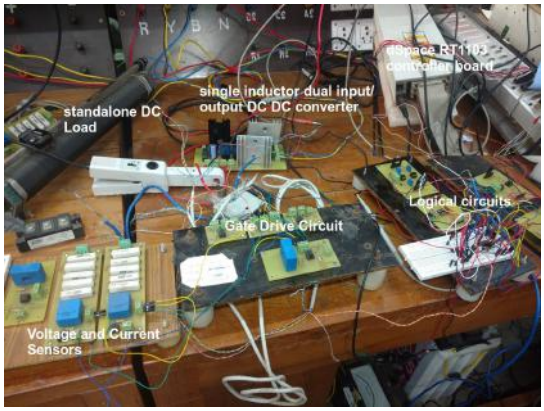

Fig. 13. Experimental Setup of the power flow management system

3) Case III: Change in mode from DOBM to DIBM due to deficit power : The power flow management system is initially operating at DOBM with solar PV power of 36 W ($600W/m^2$). At the time instant t_{spv2} shown in Fig. 12, the solar insolation level is decreased to 300 W/m^2, which results in power deficit. The MPPT algorithm adjusts the duty ratio d_{MPPT} ($= d_{S_{boost}}$) to reach the new MPP. The deficit results in a fall in v_o. The voltage controller compensates by increasing the duty ratio d_{Volt} (=d_{D1}) to regulate load voltage. This in turn results in gradual decrease of duty ratio d_{S2} to zero and corresponding reduction of power flow to the battery to zero. At this point, voltage control is lost. This combined with fall in DC load voltage v_o below V_o^* is used by the mode change control to shift the converter to DIBM. In DIBM, the voltage control signal d_{Volt} is routed to $d_{S_{boost}}$ and it increases the voltage to V_o^*.

B. Experimental Results

The single inductor based dual input/output DC-DC converter in the power flow management system was fabricated by using MOSFET switches (IRF540N) rated at 23 A, 100 V and diodes (body diode of IRF540N) rated at 23 A. Three 24 V 60 W solar PV module were used as power sources and resistive standalone DC load was used. A 36 V 40 Ah lead acid battery is used as energy storage. The input capacitor C_{in} and DC load capacitor C_o were rated at 1000μF. A 100μH toroidal inductor rated at 20 A is used. The converter is switched at 100 Khz. The controller is

This article has been accepted for publication in a future issue of this journal, but has not been fully edited. Content may change prior to final publication. Citation information: DOI 10.1109/TPEL.2018.2804658, IEEE Transactions on Power Electronics

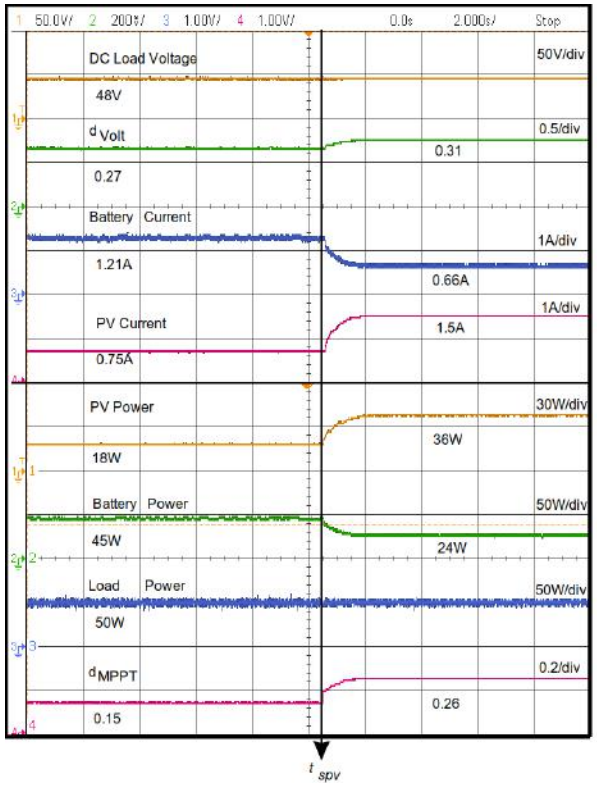

Fig. 14. Experimentation Case I: Dynamic response of the converter to changes in solar PV insolation

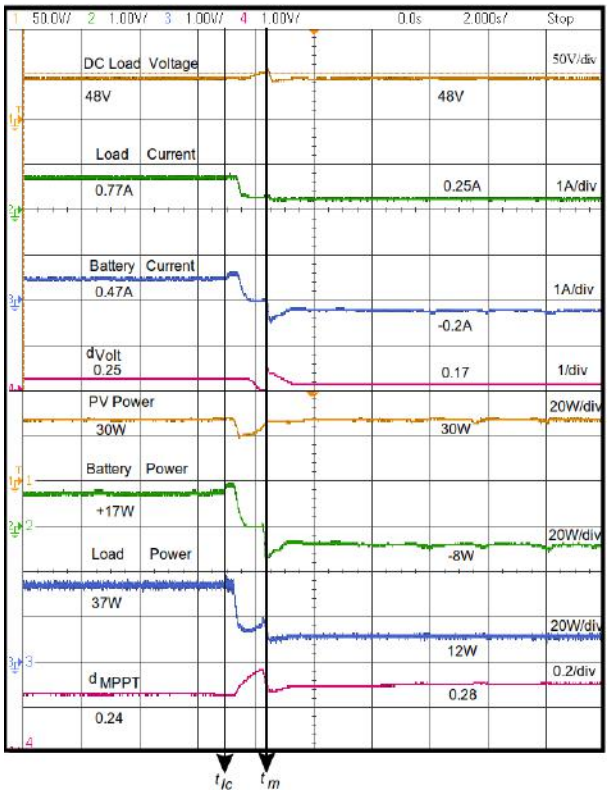

Fig. 15. Experimentation Case II: Dynamic response of the converter to changes in load

implemented by using MATLAB/Simulink programming and the generated code is dumped into the dSPACE DS1103 RTI board. The feedback is achieved by using LV 25-p voltage and LA 55-p current sensors. A passive low pass filter with a corner frequency of 1 Khz is used to eliminate noise in the feedback circuit. The PI controller parameters are k_p=0.5 and k_i=8. The power quantities P_{load}, P_{bat} and P_{pv} are computed inside the dSPACE DS1103 Real Time Interface board and recorded in a DSO. The gate pulses are generated by using dSPACE DS1103 RTI board and XOR logic gate. The gate pulses are then fed to LM339, a quad package comparator which acts as a buffer between the dSPACE DS1103 RTI board and HCPL-3120 optocouplers. The optocouplers are then interfaced with appropriate switches. The experimental setup is shown in Fig.13.

1) Case I: Dynamic response of the converter due to increase in solar PV input from 18 W to 36 W: The converter is operating at DIBM with both solar PV and battery satisfying a standalone DC load demand of 50 W. At time instant t_{spv} as shown in Fig. 14, the solar PV input was doubled to 36 W. The MPPT controller increases d_{MPPT} to shift the solar PV to the new MPP. The voltage controller increases d_{Volt} as the effective input voltage as shown in equation(7) is reduced due to increase in d_{Din}. Due to increase in d_{Din} (equation 13), d_{S3} (equation 14) decreases and hence the power drawn from the battery decreases.

2) Case II: Mode change to DOBM due to decrease in standalone DC load from 37 W to 12 W: The standalone DC load power demand was 37 W, which is supplied by both solar PV and battery with the converter in DIBM . At time instant t_{lc} as shown in Fig.15, the standalone DC load power demand is reduced to 12 W. Due to surplus power, the voltage increases. The voltage controller reduces d_{Volt}. After it reaches equal to d_{MPPT}, the MPPT control takes over control of switch S_3, which results in loss of voltage control. The mode change control then shifts the converter from DIBM to DOBM at time t_m to divert surplus power to charge the battery bank. The voltage control is now restored and the standalone DC load voltage is regulated to V_o^*.

3) Case III: Mode change to DIBM due to decrease in solar PV input from 36 W to 18 W: The converter is operating at DOBM with a standalone DC load power demand of 20W and solar PV input of 36 W. At time instant t_{spv} as shown in Fig. 16, the solar PV input is halved from 36 W to 18 W. Since the standalone DC load power demand is 20 W, this results in deficit power and decrease in v_o. The MPPT control decreases d_{MPPT} to shift to the new MPP. The voltage controller increases d_{Volt} to compensate for drop in v_o, but this is not enough. The mode change control shifts the converter from DOBM to DIBM at time t_m to use the battery as an additional power source to make up for the power deficit. The voltage controller then regulates d_{Volt} to bring v_o to V_o^*.

The converter is also operated under several more levels of solar PV power and load demand as shown in TABLE II. The different levels of solar PV power are obtained by changing the number of solar PV panels in parallel.

The simulation and experimental results proves the efficacy

This article has been accepted for publication in a future issue of this journal, but has not been fully edited. Content may change prior to final publication. Citation information: DOI 10.1109/TPEL.2018.2804658, IEEE Transactions on Power Electronics

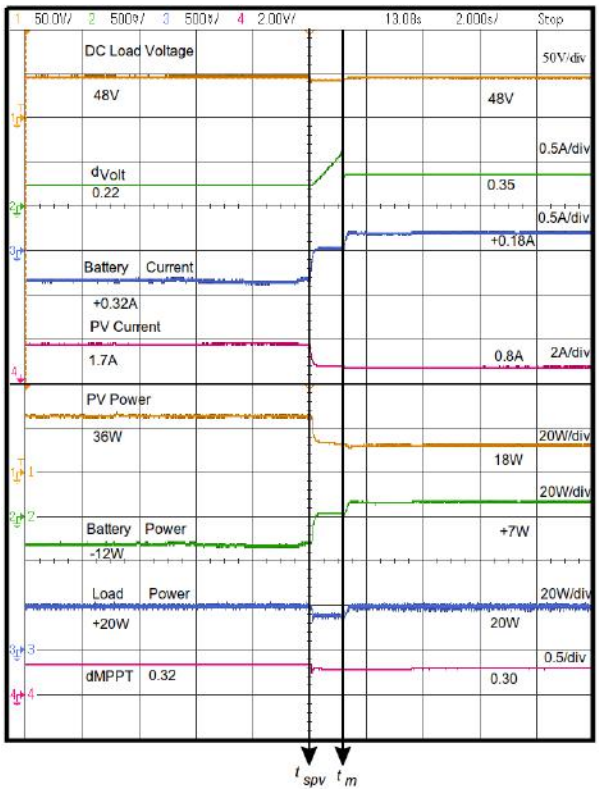

Fig. 16. Experimentation Case III: Dynamic response of the converter to changes in solar PV insolation

of the proposed power flow management system for standalone solar PV applications.

VI. Conclusion

A power flow management system for battery backed standalone solar PV systems employing single stage single inductor dual input/output DC-DC converter has been presented. A novel time sharing voltage mode control scheme has been proposed for power flow management between solar PV, battery and DC loads to maintain constant DC load voltage and also extract maximum power from solar PV. The converter is capable of operating both in surplus and deficit PV power. A hardware prototype of the proposed system consisting of solar PV, the single inductor based dual input/output DC-DC converter and a battery bank has been fabricated and the control circuits has been implemented on a dSPACE DS1103 Real Time Interface(RTI) board.

The steady state operation of both the dual output boost mode and dual input boost mode has been simulated and validated using the MATLAB programming language and the characteristics are presented. A state space average model of the proposed system was developed to perform transient analysis of the system. Simulated waveforms of the PV current, the standalone DC load voltage, the standalone DC load current, the averaged battery current, the solar PV power, the battery power and the standalone DC load power were obtained using this model are shown for changes in levels of incident solar insolation and DC load on the system. These dynamic changes were also carried out in the experimental setup and the waveforms of the corresponding electrical quantities were captured in the DSO and are presented. The simulation and and experimental performance presented confirms the satisfactory working of the controller in maintaining the desired DC load voltage, under the varying operating conditions of solar PV insolation and consumer load.

Acknowledgment

The authors would like to thank the authorities of the National Institute of Technology, Tiruchirappalli, India for all the facilities provided for carrying out the experimental and simulation work at the Switched Mode Power Conversion Research Laboratory for the preparation of this paper.

References

[1] X. Liu and E. Sánchez-Sinencio, "A highly efficient ultralow photovoltaic power harvesting system with mppt for internet of things smart nodes," *IEEE Transactions on Very Large Scale Integration (VLSI) Systems*, vol. 23, no. 12, pp. 3065–3075, Dec. 2015.

[2] M. Ito, K. Kato, H. Sugihara, T. Kichimi, J. Song, and K. Kurokawa, "A preliminary study on potential for very large-scale photovoltaic power generation (vls-pv) system in the gobi desert from economic and environmental viewpoints," *Solar Energy Materials and Solar Cells*, vol. 75, no. 3-4, pp. 507–517, 2003, {PVSEC} 12, {PART} {III}.

[3] C. D. Xu and K. W. E. Cheng, "A survey of distributed power system - ac versus dc distributed power system," in *2011 4th International Conference on Power Electronics Systems and Applications*, Jun. 2011, pp. 1–12.

[4] X. Sun, Y. Shen, W. Li, and H. Wu, "A pwm and pfm hybrid modulated three-port converter for a standalone pv/battery power system," *IEEE Journal of Emerging and Selected Topics in Power Electronics*, vol. 3, no. 4, pp. 984–1000, Dec. 2015.

[5] Y. C. Liu and Y. M. Chen, "A systematic approach to synthesizing multi-input dc-dc converters," *IEEE Transactions on Power Electronics*, vol. 24, no. 1, pp. 116–127, Jan. 2009.

TABLE II
Operation of the Proposed System under various levels of solar PV power and output DC load demand with a battery of 36 V DC and output voltage of 48 V DC

No. of Panels	I_{pv}, A	P_{pv}, W	I_{bat}, A	P_{bat}, W	I_o, A	P_{load}, W	Mode
1	1.04	25	0.7	28	0.94	45	DIB
1	0.62	15	0.244	9	0.42	20	DIB
2	1.64	40	-0.49	-18	0.313	15	DOB
3	3.72	90	-0.7	-26	1.04	50	DOB
2	3.09	75	0.84	31	1.88	90	DIB

[6] Y. M. Chen, A. Q. Huang, and X. Yu, "A high step-up three-port dc-dc converter for stand-alone pv/battery power systems," *IEEE Transactions on Power Electronics*, vol. 28, no. 11, pp. 5049–5062, Nov. 2013.

[7] O. Ray, A. P. Josyula, S. Mishra, and A. Joshi, "Integrated dual-output converter," *IEEE Transactions on Industrial Electronics*, vol. 62, no. 1, pp. 371–382, Jan. 2015.

[8] H. Wu, J. Zhang, and Y. Xing, "A family of multiport buck-boost converters based on dc-link-inductors (dlis)," *IEEE Transactions on Power Electronics*, vol. 30, no. 2, pp. 735–746, Feb. 2015.

[9] W.-H. Ki and D. Ma, "Single-inductor multiple-output switching converters," in *Power Electronics Specialists Conference, 2001. PESC. 2001 IEEE 32nd Annual*, IEEE, vol. 1, 2001, pp. 226–231.

[10] S. Bandyopadhyay and A. P. Chandrakasan, "Platform architecture for solar, thermal, and vibration energy combining with mppt and single inductor," *IEEE Journal of Solid-State Circuits*, vol. 47, no. 9, pp. 2199–2215, Sep. 2012.

[11] L. Benadero, V. Moreno-Font, R. Giral, and A. E. Aroudi, "Topologies and control of a class of single inductor multiple-output converters operating in continuous conduction mode," *IET Power Electronics*, vol. 4, no. 8, pp. 927–935, Sep. 2011.

[12] W. Jiang and B. Fahimi, "Multiport power electronic interface – concept, modeling, and design," *IEEE Transactions on Power Electronics*, vol. 26, no. 7, pp. 1890–1900, Jul. 2011.

[13] Y. J. Moon, Y. S. Roh, J. C. Gong, and C. Yoo, "Load-independent current control technique of a single-inductor multiple-output switching dc-dc converter," *IEEE Transactions on Circuits and Systems II: Express Briefs*, vol. 59, no. 1, pp. 50–54, Jan. 2012.

[14] A. Nami, F. Zare, A. Ghosh, and F. Blaabjerg, "Multi-output dc-dc converters based on diode-clamped converters configuration: Topology and control strategy," *IET Power Electronics*, vol. 3, no. 2, pp. 197–208, Mar. 2010.

[15] A. Khaligh, J. Cao, and Y.-J. Lee, "A multiple-input dc–dc converter topology," *IEEE Transactions on power electronics*, vol. 24, no. 3, pp. 862–868, 2009.

[16] Z. Rehman, I. Al-Bahadly, and S. Mukhopadhyay, "Multiinput dc–dc converters in renewable energy applications–an overview," *Renewable and Sustainable Energy Reviews*, vol. 41, pp. 521–539, 2015.

[17] M. H. Huang and K. H. Chen, "Single-inductor multi-output (simo) dc-dc converters with high light-load efficiency and minimized cross-regulation for portable devices," *IEEE Journal of Solid-State Circuits*, vol. 44, no. 4, pp. 1099–1111, Apr. 2009.

[18] H. Shao, X. Li, C. Y. Tsui, and W. H. Ki, "A novel single-inductor dual-input dual-output dc-dc converter with pwm control for solar energy harvesting system," *IEEE Transactions on Very Large Scale Integration (VLSI) Systems*, vol. 22, no. 8, pp. 1693–1704, Aug. 2014.

[19] E. Babaei and O. Abbasi, "Structure for multi-input multi-output dc-dc boost converter," *IET Power Electronics*, vol. 9, no. 1, pp. 9–19, 2016.

[20] H. Keyhani and H. A. Toliyat, "A zvs single-inductor multi-input multi-output dc-dc converter with the step up/down capability," in *2013 IEEE Energy Conversion Congress and Exposition*, Sep. 2013, pp. 5546–5552.

[21] M. A. G. de Brito, L. Galotto, L. P. Sampaio, G. d. A. e Melo, and C. A. Canesin, "Evaluation of the main mppt techniques for photovoltaic applications," *IEEE Transactions on Industrial Electronics*, vol. 60, no. 3, pp. 1156–1167, Mar. 2013.

[22] A. Luque and S. Hegedus, *Handbook of photovoltaic science and engineering*. John Wiley & Sons, 2011.

[23] M. R. Jongerden and B. R. Haverkort, "Which battery model to use?" *IET Software*, vol. 3, no. 6, pp. 445–457, Dec. 2009.

Anand I is a Research Scholar in National Institute of Technology, Tiruchirappalli, pursuing his PhD degree. He has completed his Bachelors in Electrical and Electronics Engineering at PSG Tech and Masters in Power electronics at SSN college of Engineering, India. He has been working in the area of renewable energy applications since 2014.

Subramaniam Senthilkumar(M'17) has completed his B.E. in Electrical and Electronics Engineering at Madurai Kamarajar University, India at 1999, M.Tech. in Electrical Drives and Control at Pondicherry University at 2005. He has obtained his PhD in electrical engineering at National Institute of Technology, Tiruchirappalli. He has 17 years of teaching experience at various engineering institutions. From April 2006, he is working as assistant professor in National Institute of Technology Tiruchirappalli. He has extensively researched in self excited induction generator for standalone and grid connected applications. Also, he is currently doing research in developing new power converter topologies for renewable energy systems.

Deepankar Biswas completed his B.Tech. in Electrical and electronics engineering in Jalpaiguri Government Engineering College at 2014. He finished his M.Tech. in Power Electronics at National Institute of Technology, Tiruchirappalli at Jun 2016. He has worked in the area of power converters for renewable energy systems. He is currently working in Indian Oil Corporation Limited.

M. Kaliamoorthy received his bachelor in Electrical and Electronics Engineering from Madras University in 1999 and received his post graduation in Electrical Drives and Control from Pondicherry University in 2006. He started his research in the year 2011 in the area of grid connected multilevel inverters and completed his PhD in the year 2015 from Anna University, Chennai. He is a gold medalist in his post graduate programme from Pondicherry University for the academic year 2005-2006. He has nearly 16 years of teaching experience. Since 2016 he is working as Associate Professor in the Department of Electrical and Electronics engineering at Dr. Mahalingam College of Engineering and Technology, Pollachi, Tamilnadu, India. His research interests includes multilevel inverter, power electronics for renewable energy systems